Three-dimensional Heisenberg spin-glass behavior in $SrFe_{0.90}Co_{0.10}O_{3.0}$

J. Lago,[1,*] S. J. Blundell,[2] A. Eguia,[1] M. Jansen,[3] and T. Rojo[1]

[1]*Departament of Inorganic Chemistry, Universidad del País Vasco (UPV-EHU), E-48080 Bilbao, Spain*

[2]*Clarendon Laboratory, Department of Physics, University of Oxford, Oxford OX1 3PU, United Kingdom*

[3]*Max-Planck-Institut für Festkörperforschung, D-70569 Stuttgart, Germany*

(Received 30 March 2012; revised manuscript received 13 July 2012; published 7 August 2012)

The series $SrFe_{1-x}Co_xO_3$ evolves from spiral antiferromagnetic order to long-range ferromagnetism on increasing Co doping. In the Fe-rich region below the onset of ferromagnetism ($x \leqslant 0.20$), there exists a number of disordered magnetic ground states. Here we present a detailed study of the composition $SrFe_{0.90}Co_{0.10}O_3$, which we find to display quasicanonical spin-glass behavior. The analysis of its freezing transition by means of muon spin relaxation (μSR) spectroscopy and ac and dc susceptibility suggests that the system constitutes a new experimental realization of the three-dimensional Heisenberg spin-glass model with weak random anisotropy. The derived critical exponents are consistent with predictions by Kawamura's chiral driven freezing scenario with a bimodal exchange distribution.

DOI: 10.1103/PhysRevB.86.064412 PACS number(s): 75.50.Lk, 75.40.Cx, 75.40.Gb, 76.75.+i

I. INTRODUCTION

Following the large body of evidence that shows that magnetoelectronic phase separation at the nanoscale is at least partially responsible for much of the observed phenomenology in the CMR manganites, the cobaltites or even the high-T_c cuprates,[1,2] we have embarked in a systematic study of the series $SrFe_{1-x}Co_xO_{3.0}$ (SrFeCo), a system that has so far received much less attention than the former despite early indications of a complex phase diagram[3] and the report of large negative magnetoresistance for $x = 0.10$.[4] In this series, an evolution from antiferro- to ferromagnetic behavior has been reported on increasing Co doping, with inhomogeneous ground states suggested for $x < 0.20$.[5] $SrFeO_{3.0}$ ($x = 0$) is a metallic antiferromagnet ($T_N = 134$ K) with a helicoidal spin structure.[6] The electronic ground state in this material is dominated by a $d^5\underline{L}$ configuration (where $\underline{L}$ is an oxygen hole)[7] as a result of a negative charge transfer gap character. The strong Fe $3d$–O $2p$ hybridization that occurs as a consequence gives rise to an extended σ^* band of e_g parentage in which charge carriers are holes in mainly oxygen levels. The compound thus shows metallic conductivity. The helical magnetic structure is commonly accepted to arise from the competition between antiferromagnetic exchange coupling between localized t_{2g} spins and ferromagnetic double-exchange interactions induced by the delocalized oxygen holes. Recent calculations, however, have challenged this view and shown that double exchange alone may be sufficient to generate it.[8] At the other end of the series, $SrCoO_{3.0}$ ($x = 1$) is also a charge transfer material with a negative gap.[9] The system is metallic and ferromagnetic ($T_c = 280$ K)[5,9] with a Co electronic state that is dominated by a $d^6\underline{L}$ ($t_{2g}^4 e_g^2\underline{L}$) configuration. How the enhanced delocalization of the Fe e_g electrons that occurs on Co substitution[5] causes the observed strengthening of ferromagnetic interactions along the series is not yet completely understood. As indicated by Abbate and co-workers,[10] the intuitive strengthening of the double-exchange interactions may not provide the right mechanism for ferromagnetism in this family due to the large difference in the potential felt by the e_g electrons at the Fe and Co sites. Instead, these authors propose a picture of half-metallic ferromagnetism in which Co doping induces a gap at the Fermi level in the majority e_g band thus turning the system ferromagnetic.

The composition $x = 0.20$ has been taken to mark the onset of long-range ferromagnetism in the series. Recently, we have shown that long-range ordering does indeed set in below ca. 240 K in this material although the ground state is far from being that of a conventional ferromagnet. Instead, at T_c, only about a third of the iron moments participate in the percolating FM cluster, the rest remaining nonmagnetic.[11] Even at temperature as low as 77 K almost 30% of the total spins are still paramagnetic-like according to Mössbauer measurements.[12]

For lower Co content, competing ferro- and antiferromagnetic interactions are claimed to generate inhomogeneous magnetic behavior in the Fe-rich region.[5,13] Here we present a detailed study of $SrFe_{0.90}Co_{0.10}O_{3.0}$ and show that, for this composition, the system behaves at low temperature as a quasicanonical spin glass with only a small degree of spin clustering. Thus, at about 80 K, it undergoes a freezing transition whose analysis suggests three-dimensional (3D) Heisenberg critical behavior.

II. EXPERIMENTAL DETAILS AND METHODS

Polycrystalline samples of $SrFe_{0.9}Co_{0.1}O_{3.0}$ were synthesized following the ceramic method described elsewhere.[11] The quality and phase purity of the samples were determined by high resolution neutron diffraction using the HRPD diffractometer at ISIS (RAL, UK). Ac susceptibility was measured on a Lakeshore susceptometer while dc measurements were performed with a Quantum Design SQUID magnetometer. Zero-field (ZF) muon spin relaxation (μSR) measurements were performed at the SμS facility at PSI (Switzerland). A brief description of these measurements was given in Ref. 11; for a more detailed account on the technique see, for example, Ref. 14

III. RESULTS AND DISCUSSION

Figure 1 shows the temperature dependence of the dc susceptibility for $SrFe_{0.9}Co_{0.1}O_{3.0}$ in an applied field of

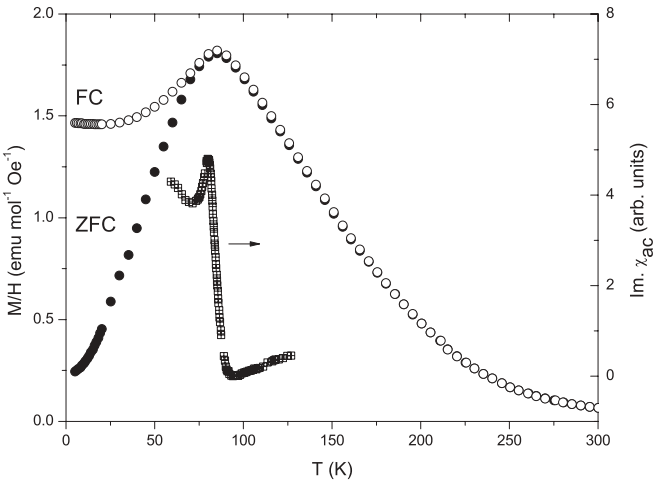

FIG. 1. (Left axis) Zero-field cooled (solid circle) and field-cooled (open circle) dc-susceptibility data for $SrFe_{0.9}Co_{0.1}O_{3.0}$ in $h_{appl} = 100$ Oe. (Right axis) Imaginary part (open square) of the ac susceptibility measured in 153 Hz.

100 Oe. Consistent with previous reports,[5] a peak centered at $T_f \simeq 80$ K marks the freezing of the Fe/Co moments into a glassy state below this temperature. This peak is accompanied by the onset of remanence effects—marked by the divergence of the zero-field-cooled (ZFC) and field-cooled (FC) curves—and a sharp rise in the imaginary part of the ac susceptibility χ'' (Fig. 1, right). Both features are consistent with the onset of nonequilibrium behavior and are characteristic of a transition into a frozen spin-glass state. However, in principle, they could also be signaling a dynamic blocking of superparamagnetic-like clusters, which, taking into consideration the electronic phase separation found in the $x = 0.20$ member of this family,[11] constitutes a real possibility in the present material. In fact, the strong deviation from a Curie-Weiss law below temperatures as high as $3T_f$ indicate the existence of strong ferromagnetic spatial correlations in the system ($\theta \simeq 230$ K from a fit of the experimental data above 250 K; not shown). Thus, in order to definitively establish the nature of the freezing process and therefore of the low-temperature phase in $SrFe_{0.9}Co_{0.1}O_{3.0}$, a study of its static and dynamic behavior has been performed in the vicinity of T_f, the results of which are outlined in the following sections.

A. Spin dynamics near and below freezing

1. μSR results

Figure 2 shows a few characteristic μSR spectra for $SrFe_{0.8}Co_{0.1}O_{3.0}$ at temperatures above and below T_f. The red solid lines are the fit to a power exponential function $P_z(t) = A_r \exp[-(\lambda t)^s)] + b_k$, where λ(T) is the dynamic muon spin depolarization rate due to fluctuations in the internal dipolar field sensed by the muon inside the powder sample, b_k is a background term that accounts for muons stopped outside the sample, and $A_0 = A_r + b_k$ is the full resolved asymmetry of the signal. Note that the usual β exponent has been renamed as s in order to avoid confusion with the critical exponent in the analysis below.

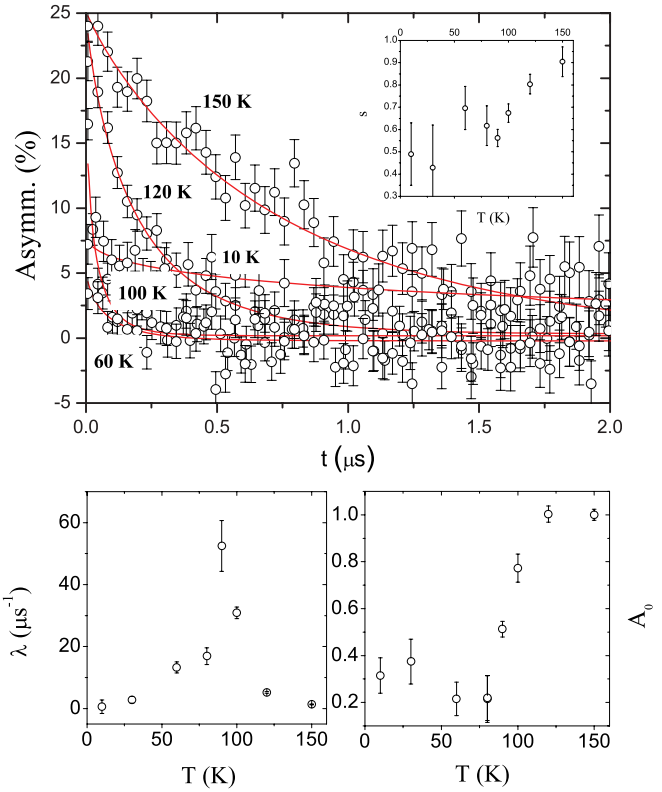

FIG. 2. (Color online) (Top) Zero-field muon spin relaxation spectra for $SrFe_{0.9}Co_{0.1}O_{3.0}$ at various characteristic temperature spanning the freezing transition. (Inset) Temperature dependence of the power s in $P_z(t) = A_r \exp[-(\lambda t)^s)] + b_k$. (Bottom) Temperature dependence of the muon relaxation rate $\lambda(T)$ (left), showing the slowing down of spin fluctuations on approaching the transition, and of the normalized muon asymmetry A_0(norm.) $= A_0(T)/A_0$(high T) (right). Consistent with expectations for a spin-glass system with large magnetic moments, below T_f the asymmetry falls to about 1/3 of its value in the paramagnetic state.

Well above T_f the depolarization is exponential (i.e., $s \simeq 1$), meaning that electronic spin dynamics are rapid and characterized by a single spin-spin correlation time τ_c. In this temperature range, $\lambda \propto \gamma_\mu^2 \Delta^2 \tau_c$, where Δ is the second moment of the internal field distribution and $\gamma_\mu = 135.5$ MHzT^{-1} is the muon gyromagnetic ratio. $\lambda(T)$ thus reflects the T evolution of the average correlation time and, as expected, raises as $T \to T_f^+$ signaling the critical slowing down of spin fluctuations. However, as T is lowered towards the transition the relaxation becomes nonexponential (i.e., s departs from unity), reflecting instead a spread of correlation times, which, above T_f, can be associated with a certain degree of spin clustering (i.e., inhomogeneous phase separation). Below T_f, nonexponential behavior is a natural consequence of the random spin freezing expected for in the frozen state of conventional spin glasses. Note that, even considering the limitations imposed to any quantitative conclusion by the large error associated with s at low temperatures (which reflects the difficulty in fitting the fast depolarization of the muon ensemble that takes place at very early times), the mean fitted values of the exponent are clearly above the value of 1/3 predicted by theory for a dense spin system.[15] We do not

have at the moment an explanation for this behavior but it could be related to the clustering we detect in the susceptibility measurements described below.

For a spin-glass system below the freezing temperature, the μSR signal is characterized by a rapid depolarization of 2/3 of the initial asymmetry followed by the slower relaxation of the residual 1/3 tail. This reflects a broad distribution of internal fields seen by the muon, a consequence of the freezing of the magnetic moments in random patterns that remain quasistatic in the time scale of the muon lifetime ($\sim$2.2 μs). In our case, the large size of the Fe/Co(IV) moment makes the initial damping of the 2/3 transverse component too fast to be detected experimentally, and so, for $T \leqslant T_f$, the signal is reduced to the relaxing 1/3 longitudinal tail (Fig. 2, bottom right). The flattening of this component that occurs on cooling reflects the gradual decrease of $\lambda(T)$ below T_f as the density of low energy excitations decays towards zero as $T \rightarrow 0$ (Fig. 2, bottom left).

2. *Nonequilibrium spin dynamics below T_f*

The observation of extremely slow relaxation processes is another key feature characterizing the frozen state in real spin glasses. It results from the rugged "multivalley" energy landscape that develops below freezing with metastable states (valleys) separated by barriers whose heights grow with decreasing temperature.[16] Thus, cooling the system through T_f gets it stuck in one such valley, from which it can only evolve by "jumping" the barriers that separate it from adjacent states. The large variance of barrier heights and the fact that some diverge at any temperature below T_f results in that a spin glass displays, at low temperature, relaxation processes at *all* time scales, from the microscopic spin flip ($\propto 10^{-12}$ s in canonical systems) to the macroscopic experimental times. In particular, the response to a small excitation (such as a change in the applied field) is extremely slow below T_f and, as in other glassy materials, depends on the *waiting time* t_w that the system spends in the low T phase before the excitation is applied ("*aging*").[17]

Various experimental ac- and dc-cycling procedures are usually employed to study nonequilibrium dynamics—and in particular aging—in spin glasses.[18] Of these, we have chosen the simple zero-field-cooled magnetization (ZFCM) method in order to corroborate the existence of aging phenomena in $SrFe_{0.8}Co_{0.1}O_{3.0}$. In the ZFCM method, the time evolution of the magnetization is measured after (i) cooling the sample from a high temperature above the transition to $T_{\rm exp} < T_f$ in zero applied field and (ii) waiting a time t_w at $T_{\rm exp}$ before the excitation (a small dc field within the linear response regime) is applied. In our study, $h_{\rm dc} = 20$ Oe, $T_{\rm exp} = 40$ K ($\approx 0.5 T_f$) and $t_w = 100$, 1000 and 5000 s.

The results are plotted in Fig. 3. The slow evolution of the magnetization with time, as shown by the curves in Fig. 3(a) (where the magnetization is presented as $\Delta M = M(t)$-$M(0)$], with no saturation in the time scale of the measurements, is a clear indication of slow glassy dynamics below T_f. The change in their shape, with an inflexion point that occurs at longer observation times with increasing t_w [Fig. 3(a)] reveals, in turn, an age-dependent phenomenon. This is best observed in the plot in Fig. 3(b) of the relaxation rate $S(t) \equiv \partial M(t)/\partial \log t$ vs time. The curves show a maximum at the value of t at which

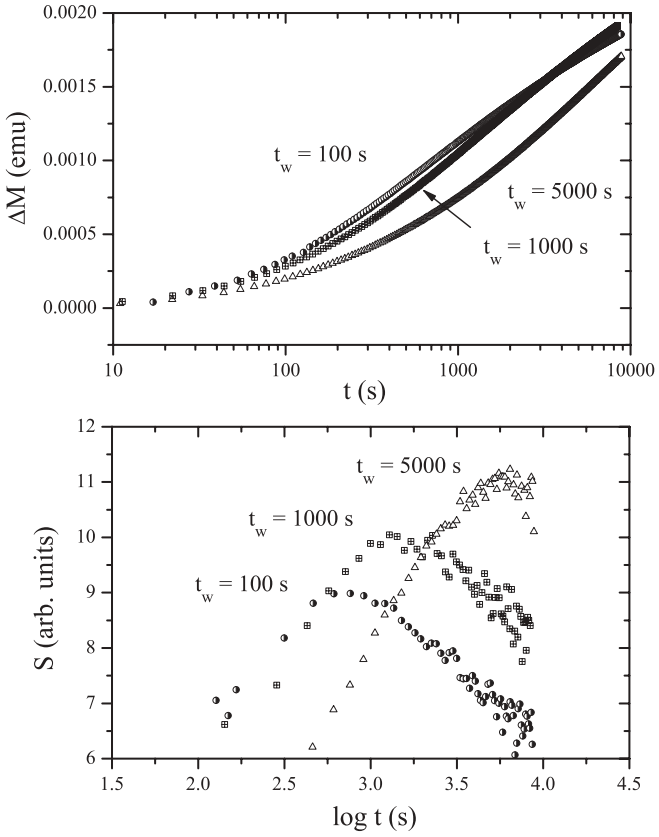

FIG. 3. (a) Time evolution of the ZFC magnetization, expressed as $\Delta M = M(t)$-$M(0)$ and (b) the corresponding relaxation rate $S(t) \equiv \partial M(t)/\partial \log t$ measured at $T_{\rm exp} = 40$ K in a field $h = 20$ Oe after waiting for $t_w = 100$, 1000, and 5000 s in zero field at the experimental temperature.

the inflexion points in the $M(t)$ curves are observed. Note that the $S(t)$ maxima do not occur at $t = t_w$ but at $t_{\rm eff} > t_w$, where $t_{\rm eff}$ is the true waiting time the system experiences and that results from the addition to the nominal value the time it takes for the system to thermalize and stabilize at the set experimental temperature and field values. In any case, the presence of these maxima in the $S(t)$ curves is a clear signature of aging and, thus, of nonequilibrium dynamics in the system. The phenomenon is, as mentioned above, characteristic of the frozen low temperature phase of "atomic" spin glasses, where has been traditionally explained within the "droplet model" of Fisher and Huse.[19] However, it is not exclusive to them. Ample evidence exists in the literature of such behavior in cluster glasses[20] and superspin glasses,[21] in which, although collective relaxation exists, the freezing is not understood in terms of a thermodynamic phase transition. Hence, the plots in Fig. 3, signaling aging dynamics in $SrFe_{0.8}Co_{0.1}O_{3.0}$, are *only* consistent with a spin-glass transition but could not, on their own, be considered as definitive proof of it.

3. *ac-χ results*

In order to further characterize the nature of the transition in $SrFe_{0.9}Co_{0.1}O_{3.0}$, its dynamic critical behavior was also studied by means of ac-susceptibility measurements as a function of the frequency (66–1000 Hz) of the driving ac field. The relative variation of the freezing temperature [determined from the

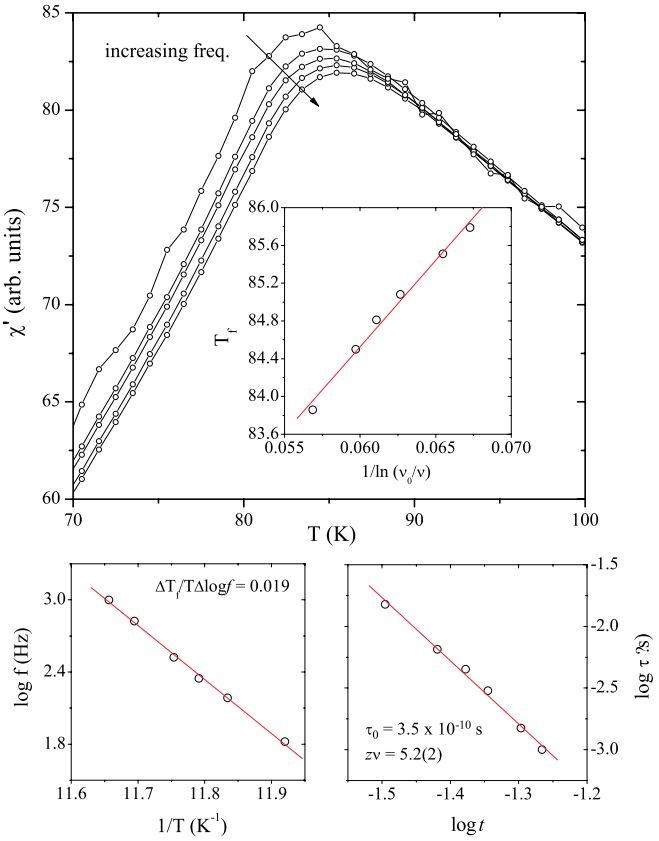

FIG. 4. (Color online) (Top) Temperature dependence of in-phase ac susceptibility for different frequencies (66–1000 Hz) of the driving field. (Inset) Vogel-Fulcher representation of the frequency dependence of the freezing temperature. The solid line is the fit to Eq. (2). (Bottom) Frequency dependence of the freezing temperature plotted as log f vs $1/T$ in order to determine the relative variation by frequency decade (left). Log-log plot of the characteristic time $\tau = 1/f$ vs reduced temperature t; from which the critical exponent $z\nu$ is derived (right).

cusp of the real component χ' (Fig. 4)] per frequency decade $\Delta T_f/(T_f \Delta \log(\omega))$ is 1.9×10^{-2}, intermediate between canonical spin glass[22] and superparamagnetic behavior, for which strong frequency sensitivity is expected.[16,22] Similar values have been reported for cluster glass systems, in which the low temperature spin-glass-like phase is due to interactions between spin clusters rather than independent spins.[23] It is therefore worth considering the possibility that, as in those cases, some degree of clustering exists also in $SrFe_{0.9}Co_{0.1}O_{3.0}$ and the freezing is thus a dynamic blocking process rather than a true thermodynamic transition. In view of the critical analysis below, however, let us consider first the true equilibrium transition scenario. In this case, the slowing down of electronic spin dynamics that occurs when the freezing point is approached from above reflects the divergence of the correlation time τ according to $\tau \propto \xi^z$, where ξ and z are the correlation length and the dynamical scaling exponent, respectively.[24] The correlation length in turn diverges with temperature as $\xi \propto t^{-\nu}$ and so, the evolution of the correlation time near the critical point is given by the power law,

$$\tau = \tau_0 t^{-z\nu}, \tag{1}$$

where τ_0 is the characteristic time of a single spin (or fluctuating entity) flip. In our case, a log-log plot of τ (obtained as the inverse of the experimental frequency) vs reduced temperature is shown in Fig. 4 (bottom, right). The red solid line is the fit to Eq. (9) (with T_f fixed to 81.4 K in order to minimize the large error introduced by the small number of data points), which yields $z\nu = 5.2(2)$ and $\tau_0 = 3.5(9) \times 10^{-10}$ s. Whereas the derived value of the exponent is within the range reported for well-established spin-glass systems, the characteristic time is somewhat larger than expected (in canonical spin glasses it is of order 10^{-12}–10^{-13} s),[23,24] although it still remains orders of magnitude smaller than the values reported for cluster glass materials ($\tau_0 \propto 10^{-7}$ s).[23,25] According to this analysis, the freezing is thus best described as a true spin-glass continuous transition despite the slight deviation in τ_0, which probably reflects a small level of clustering not sufficiently important so as to alter the overall critical behavior.

One can nevertheless analyze the transition in $SrFe_{0.9}Co_{0.1}O_{3.0}$ in terms of the dynamic blocking of interacting clusters of spins if only for contrasting its behavior with the expected results for spin and cluster glasses. In that case, spin dynamics near the transition can be modeled according to the empirical Vogel-Fulcher law,[26]

$$\tau = 1/\nu = \tau' \exp\left(\frac{E_A}{k_B(T_f - T_0)}\right), \tag{2}$$

where τ' is, in principle, equivalent to τ_0 in Eq. (1) and T_0 is a phenomenological parameter introduced as a modification of the conventional Arrhenius expression in order to keep the value of τ' within a physical meaningful range when interactions become important between the dynamic entities. In order to fit the data, we rearrange Eq. (2) as $T_f = \frac{E_a/k_B}{\ln(\nu_0/\nu)} + T_0$ and take $\tau' = \tau_0$ derived above. This way, the activation energy E_A and T_0 can be obtained from the linear fit of the data in T_f vs $1/\ln(\nu_0/\nu)$ plot (inset of Fig. 4). The derived values are $E_A/k_B = 183(9)$ K and $T_0 = 73.6(6)$ K.

Despite the limitations of this interpretation of the spin-glass transition,[27] T_0 can be used to estimate the degree of clustering in the system. According to the criterion introduced by Tholence,[22] $\alpha = (T_f - T_0)/T_f$ should be small for spin-glass behavior. We find $\alpha = 0.1$ for $SrFe_{0.9}Co_{0.1}O_{3.0}$, in the same range as the values obtained for other well-behaved spin glasses.[28] Alternatively, the ratio between the activation energy and T_0 has also been used as a measure of the interactions between the dynamic entities freezing at T_f and thus of the level of magnetic clustering[29] (assuming a direct relation between the size of the clusters and the coupling between them). For canonical systems, $E_A/T_0 \sim 2$–3, whereas a value of 30 has been reported for a cluster glass.[29] We obtain $E_A/T_0 = 2.49$, in line again with true spin-glass behavior.

B. Static critical behavior

The above analysis of the slowing down of electronic fluctuations on approaching T_f thus points towards a true equilibrium transition rather than a thermally activated blocking process although a small degree of spin clustering might be occurring. We have therefore studied the static magnetic behavior near the transition and analyzed it in terms of the critical scaling hypothesis. For a spin glass, due to the random orientation

of the spins in the frozen low T phase, the spontaneous or staggered magnetizations or, indeed, any other parameter reflecting spatial correlations become useless to characterize a PM→SG transition. It is, instead, the squared correlation function $\langle S_i S_j \rangle^2$ that becomes long ranged below T_f, leading to the divergence of the so-called spin-glass susceptibility $\chi_{SG} = [\chi_{ij}^2]_{av} = \beta^2[(\langle S_i S_j \rangle - \langle S_i \rangle \langle S_j \rangle)^2]_{av}$.[16,30] The relevance of this is that χ_{SG} can be related[31,32] to the measurable nonlinear susceptibility, χ_{nl}, defined as the higher order contributions in the expansion of the magnetization in powers of a uniform external field, that is,

$$M = \chi H = \chi_0 H - b_3(\chi_0 H^3) + b_5(\chi_0 H^5) + \cdots,$$
$$\chi_{nl} = \chi_0 - \frac{M}{H} = b_3 H^2 - b_5 H^4 + \cdots, \tag{3}$$

with

$$\chi_{nl} = \beta^3\left(\chi_{SG} - \tfrac{2}{3}\right) \tag{4}$$

provided the series is truncated after the first nonlinear term.[16] χ_{nl} can be thus used in order to study the critical behavior at the freezing transition. In the absence of bias field-dependent measurements of the harmonics in the response to an ac field, we have used dc-magnetization isotherms collected around the transition to derive the thermal and field evolution of χ_{nl}. According to the scaling hypothesis, its behavior in the critical regime is governed by a universal equation of state, which, following Ref. 33, can be expressed as

$$M_{nl}(t,H) = \chi_{nl} H = t^{(\gamma+3\beta)/2} F(H/t^{(\gamma+\beta)/2}), \tag{5}$$

where F is an unspecified scaling function and t the reduced temperature $(T/T_f - 1)$. M_{nl} can be then expanded in powers of the applied field H as

$$M_{nl} = -b_3 t^{-\gamma} H^3 + b_5 t^{-(2\gamma+\beta)} H^5 - b_7 t^{-(3\gamma+2\beta)} H^7 + \cdots \tag{6}$$

The leading nonlinear terms χ_3 and χ_5 should thus diverge as $t^{-\gamma}$ and $t^{-2(\gamma+\beta)}$, respectively, as $t \to 0$, and this is what is observed experimentally (see the inset of Fig. 5, which shows the thermal evolution of the two coefficients derived from the fit of the magnetization to a sum of odd powers of H). The exponents β and γ can be determined through the scaling condition in Eq. (5), according to which, for the right choice of exponents, $M_{nl}/t^{(\gamma+3\beta)/2}$ data near T_f should collapse onto a single curve when plotted as a function of $H/t^{(\gamma+\beta)/2}$. The analysis was performed by an iteration method and the best scaling, shown in Fig. 5, was obtained with $T_f = 81.4(2)$, $\gamma = 1.40(1)$, and $\beta = 1.10(5)$. Their reliability can be checked by studying the asymptotic behavior of the scaling function. For temperatures significantly larger than T_f (lower part of the curve), the slope of the scaling curve tends to 3 as expected when nonlinearity diminishes and the expansion in Eq. (6) gets reduced to the first term. Close to the transition (upper part), on the other hand, the slope naturally tends to the full asymptotic value $(\gamma + 3\beta)/(\gamma + \beta)$.[33] The slope of a linear fit of the data for $t < 0.1$ (1.86) is consistent with the values of the exponents for which the collapse of the M_{nl} curves is achieved, thus corroborating their validity. Note, however, that a power law fit of the leading nonlinear term, $\chi_3 \propto t^{-\gamma}$, yields $\gamma = 3.6(1)$, significantly different from the value obtained via scaling. This

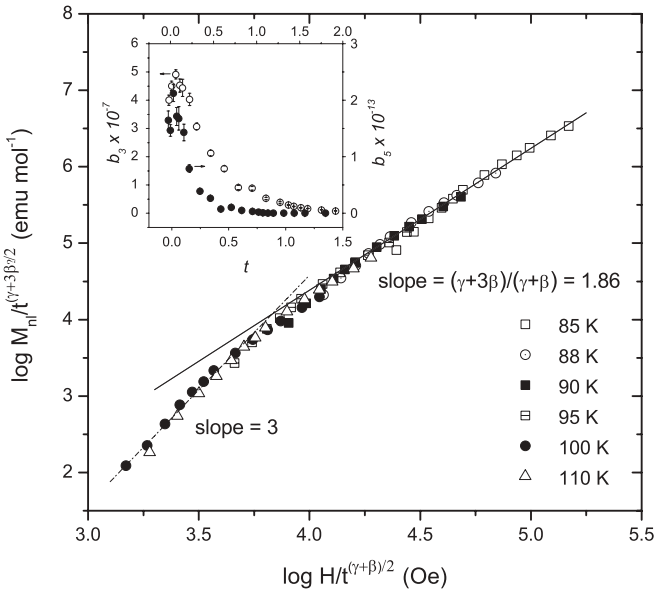

FIG. 5. Scaling plot of the nonlinear magnetization for $SrFe_{0.9}Co_{0.1}O_{3.0}$ for $t \to 0^+$ in the field range $400 < H < 3000$ Oe. The two solid lines represent the asymptotic limits of the scaling function in Eq. (5). The derived slopes are in agreement with the theory. (Inset) Temperature dependence of the coefficients of the first two terms in the expansion of the nonlinear magnetization in terms of odd powers of the applied field showing their divergence as $T \to T_f^+$.

discrepancy most likely derives from the different temperature ranges over which they are calculated, as linearity in the log-log plot of χ_3 vs t is only observed for $t \geqslant 0.6$, a range in which regular terms surely become non-negligible. We therefore take the values obtained from scaling as better estimates of β and γ. From these, the other critical exponents can be derived via the scaling and hyperscaling relations. Thus, a value of $\delta = 2.27(5)$ is obtained from $\delta = \gamma/\beta + 1$, $\alpha = -1.6$ from $\alpha + 2\beta + \gamma = 2$, and $\nu = 1.2$ from $d\nu = 2 - \alpha$, with the dimensionality $d = 3$ for the present system. The value of the exponent for the nonlinear susceptibility at T_f, δ, can in turn be "translated" into the exponent $\eta = 0.83$ via the relation $\delta = (d + 2 - \eta)/(d - 2 + \eta)$. The values of the different exponents obtained for $SrFe_{0.9}Co_{0.1}O_{3.0}$ place this material well inside the realm of the known experimental Heisenberg systems (at least in comparison with 3D Ising behavior, with much larger γ and a negative value of η).[34] However, what is most remarkable is the level of agreement of these exponents with the results of numerical simulations for the chirality driven freezing transition of Kawamura's (see below);[35] in particular with simulations with a bimodal exchange interaction distribution from which $\eta = 0.8(2)$, $\nu = 1.2(2)$, and $\gamma = 1.5(4)$ are extracted.[35]

C. Irreversibility lines: the H-T phase diagram

Figure 6 shows the ZFC and FC dc-susceptibility curves measured in $H_{appl.} = 1000$ Oe. Compared with the data in Fig. 1 ($H_{appl.} = 100$ Oe), it shows that the divergence of the FC and ZFC curves that occurs on cooling below the susceptibility maximum, shifts to lower temperature with increasing applied field. A close look at the 1000 Oe data also reveals that

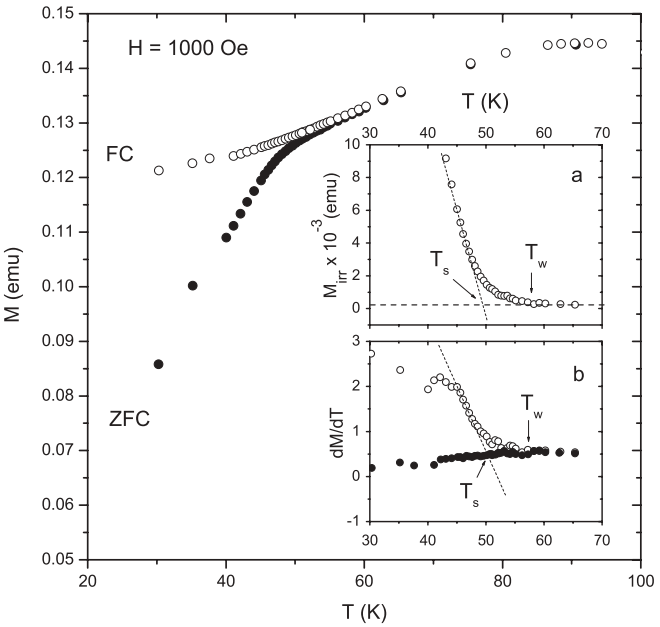

FIG. 6. Temperature dependence of the field-cooled and zero-field-cooled dc magnetization for $SrFe_{0.9}Co_{0.1}O_{3.0}$ in $H_{appl.} = 1000$ Oe. Insets a and b show the two methods described in the text to calculate the onset of weak and strong irreversibility temperatures from the irreversible magnetization (i.e., M_{FC}-M_{ZFC}).

irreversibility sets in two successive steps: In this field, weak irreversibility sets in at $T_w \simeq 60$ K, the temperature at which the FC and ZFC curves start to diverge, whereas the sudden downturn in the ZFC magnetization that occurs at $T_s \simeq 52$ K marks the onset of strong irreversibility.

The weak and strong irreversibility lines, $T_w(H)$ and $T_s(H)$, respectively, map the different stability regions in the H-T plane of a spin-glass system and their presence is predicted by the existing theoretical models. Thus, de Almeida and Thouless (AT)[36] showed that the Sherrington-Kirkpatrik (SK) solution[37] of the Edwards-Anderson (EA) model[38] in the case of infinite range interactions is unstable below a temperature T_{AT} whose evolution in an applied field has the form,

$$t_{AT}^3 = [1 - (T_{AT}(H)/T_{AT}(0))]^3 = (3/4)h^2, \qquad (7)$$

with $h = g\mu_B H/k_b T_{AT}(0)$. Experimentally, the AT line coincides with the line that separates the paramagnetic and frozen spin-glass phases in the case of Ising spins. The theory was generalized by Gabay and Toulouse (GT)[39] for an isotropic n-component vector spin glass. In this case, two successive field-dependent transitions are observed on cooling: First, the freezing occurs of the transverse spin component along the so-called GT line, a true transition line associated with the onset of weak irreversibility and expressed as

$$t_{GT} = 1 - (T_w(H)/T_w(0)) = [(n^2 + 4n + 2)/4(n + 2)^2]h^2. \qquad (8)$$

This is followed at lower temperature by the freezing of the longitudinal spin components, which takes place along a second line,

$$t_{AT'}^3 = [1 - (T_s(H)/T_s(0))]^3 = [(n + 1)(n + 2)/8]h^2. \qquad (9)$$

This line marks the crossover from weak to strong irreversibility and only becomes identical to the AT line for $n = 1$. Whether it represents a true thermodynamic phase transition is still debated and the answer to this question varies depending on the approach used to define the nature of the spin-glass phase below it: Whereas it does in Parisi's "replica symmetry breaking" (RSB) scenario,[40] it does not in the scaling or "droplet model," in which the spin-glass phase is destroyed by any finite applied field.[19]

The presence of random anisotropy (inevitable in real systems due to Dzyaloshinsky-Moriya or dipolar interactions) significantly alters the above picture. According to mean-field predictions, two extreme cases can be distinguished:[41] a strong anisotropy regime, defined for $h^{2/3} \ll d^*$ (where $d^* = D/J$, with D and J being the mean strength of the anisotropy and exchange coupling, respectively), in which the local magnetic moments behave as an Ising spin system and therefore give rise to a single, AT-like irreversibility line and a second, weak anisotropy regime ($h^{5/2} \gg d^*$), in which the behavior is akin to that of the $d^* = 0$ case; the difference is that $T_w(0)$ shifts to lower values compared to the pure isotropic situation of Eq. (8). Thus, for a vector spin glass with weak random anisotropy, a crossover from Ising to isotropic-like behavior is expected to occur with increasing applied magnetic field.

Experimentally, the H-T phase diagram obtained for numerous real spin glasses)[42] is qualitatively analogous to that predicted by the mean-field theory above even though most are closer to the 3D Heisenberg EA model, for which numerical simulations predict a zero-temperature transition already in zero field.[43] Kawamura argued that the spin-glass freezing temperature T_{SG}, if at all finite, is always lower for 3D vector spin glasses than a finite temperature (T_{CG}) at which a chiral-glass ordering transition exits that manifests itself in the presence of even weak random anisotropy[44] and is responsible for many of the experimental features in real systems.[35] The behavior of the chiral model is mean-field-like and, thus, predicts the two RSB-type transitions observed experimentally in real systems as well as the crossover from AT- to GT-like behavior on increasing applied field (for a review of the model see Ref. 45). Although the model has been contested by further calculations that argue for the existence of a single critical temperature transition involving both spin and chirality in the absence of anisotropy,[46] Kawamura's chiral picture remains an attractive explanation of why physical 3D systems follow the Heisenberg mean-field model. In particular, it predicts a similar crossover in the H-T plane albeit with a different meaning to that in the RSB theory.[47]

Results in the H-T plane for $SrFe_{0.9}Co_{0.1}O_{3.0}$ are shown in Fig. 7. The different values of the transition temperatures were obtained from ZFC-FC longitudinal magnetization measurements following the standard procedure (Fig. 6, inset a): T_w was obtained from the point at which the irreversible magnetization, $M_{irr} = M_{FC}$-M_{ZFC}, departs from zero and T_s from the extrapolation to zero of the linear part of M_{irr} in the strong irreversibility region. Alternatively, T_w and T_s can be calculated from the derivatives of M_{FC} and M_{ZFC} following the construction shown in inset b of Fig. 5.[48] The solid line in Fig. 7 is the fit of T_w to a Gabay-Toulouse power law $H = Ct_w^{1/2}$ for fields above a crossover value of ca. 100 Oe

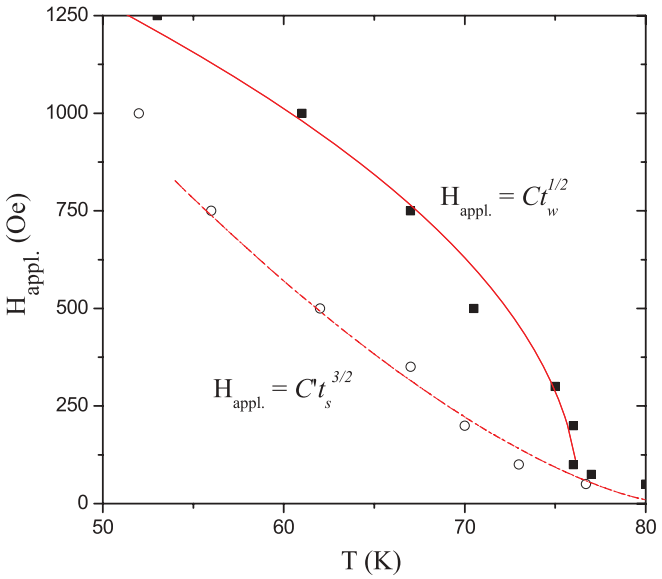

FIG. 7. (Color online) Magnetic phase diagram in the *H-T* plane for $SrFe_{0.90}Co_{0.10}O_{3.0}$. The solid and dotted lines are the fits of the weak and strong irreversibility temperatures to the Gabay-Toulouse, $H = Ct_w^{1/2}$, and d'Almeida-Thouless, $H = C't_s^{3/2}$, critical lines, respectively.

below which the weak irreversibility transition temperatures follow instead an Ising behavior and thus the d'Almeida-Thouless line. The strong irreversibility temperatures were in turn fitted to an AT-like line $H = C't_s^{3/2}$ for the entire field range (dotted line), although in this case $t_s(0)$, was fixed using the transition temperature derived from the scaling analysis [$T_s(0) = 81.4$ K]. The GT fit of the weak irreversibility line yields a zero-field transition temperature $\tilde{T}_f(0) = 76.3(2)$ K, significantly lower than the measured freezing temperature in zero field. In the mean-field model, this drift can be related to the strength of the anisotropy through[41]

$$\tilde{T}_f(0) = T_f(0) - \frac{n+2}{2(n+2)^{1/2}} \times d^*, \qquad (10)$$

yielding a value of the anisotropy parameter $d^* \simeq 4$ K. From this, making use of Fisher's expression $d^* = (\mu_B H_{cr}/k_B \tilde{T}_f(0))^{5/2} \times k_B T_f(0)$,[41] we obtain a value $H_{cr} \simeq 600$ Oe for the Ising-to-Heisenberg crossover field, significantly larger but of the same order of magnitude than the experimental one. The measured phase diagram thus appears, at least qualitatively, consistent with the RSB mean-field scenario for a Heisenberg system with weak anisotropy, which, as mentioned above, is also what would be expected from a chirality-driven transition in a 3D Heisenberg system.

IV. CONCLUSIONS

The study above the system $SrFe_{0.9}Co_{0.1}O_{3.0}$ shows that the spin freezing it undergoes at about 81 K can be understood in terms of a true equilibrium spin-glass transition and not of a dynamical blocking of spin clusters (despite a certain degree of clustering that can be detected from our data). The analysis of its critical behavior through the scaling hypothesis yields a series of critical exponents which are in agreement with what has been reported for other Heisenberg systems and, in particular, with the results of numerical simulations of the chirality-driven ordering transition scenario in three-dimensional spin glasses. The *H-T* phase diagram derived from dc-magnetization measurements is also consistent with this picture. Thus, $SrFe_{0.9}Co_{0.1}O_{3.0}$ appears as a new realization of 3D Heisenberg spin-glass behavior in an insulating material. Note that most of the known examples of this universality class are metallic alloys and, to our knowledge, such behavior in a short-range exchange insulator has only been reported before in a handful of systems including $CdCr_2InS$[42,49] and CdMnTe.[42] Further studies should be carried out on this material in order to confirm the remarkable agreement we find with the predictions of the chiral model by means of more appropriate techniques (torque[50] and Hall effect measurements). In any case, the present study provides further insight into the Fe-rich region of the magnetic phase diagram in the series $SrFe_{1-x}Co_xO_{3.0}$, which, so far, had only received limited attention despite its richness.

ACKNOWLEDGMENTS

J. Lago thanks J. Cooper (Cavendish Laboratory, University of Cambridge) and the technical staff at PSI for their assistance with the ac-susceptibility and μSR measurements, respectively. Technical support provided by SGIker (UPV/EHU, MICINN, GV/EJ, ESF) is also gratefully acknowledged. Part of this work was financially supported by the Spanish Ministerio de Educación (Project No. MAT2007-66737-C02-01).

*jorge.lago@ehu.es

[1] E. Dagotto, *Nanoscale Phase Separation and Colossal Magnetoresistance* (Springer, Berlin, 2003).
[2] J. Wu, J. W. Lynn, C. J. Glinka, J. Burley, H. Zheng, J. F. Mitchell, and C. Leighton, Phys. Rev. Lett. **94**, 037201 (2005).
[3] Y. Takeda, K. Kanno, T. Takada, O. Yamamoto, M. Takano, N. Nakayama, and Y. Bando, J. Solid State Chem. **63**, 237 (1986).
[4] P. D. Battle, M. A. Green, J. Lago, M. J. Rosseinsky, L. E. Spring, J. Singleton, and J. F. Vente, Chem. Commun. **9**, 987 (1998).
[5] S. Kawasaki, M. Takano, and Y. Takeda, J. Solid State Chem. **121**, 174 (1996).
[6] T. Takeda, Y. Yamaguchi, and H. Watanabe, J. Phys. Soc. Jpn. **33**, 967 (1972).
[7] A. E. Bocquet, A. Fujimori, T. Mizokawa, T. Saitoh, H. Namatame, S. Suga, N. Kimizuka, Y. Takeda, and M. Takano, Phys. Rev. B **45**, 1561 (1992).
[8] M. Mostovoy, Phys. Rev. Lett. **94**, 137205 (2005).
[9] R. H. Potze, G. A. Sawatzky, and M. Abbate, Phys. Rev. B **51**, 11501 (1995); P. Bezdicka, A. Wattiaux, J. C. Grenier, M. Pouchard, and P. Hagenmuller, Z. Anorg. Allg. Chem. **619**, 7 (1993).
[10] M. Abbate, G. Zampieri, J. Okamoto, A. Fujimori, S. Kawasaki, and M. Takano, Phys. Rev. B **65**, 165120 (2002).

[11] J. Lago, M. J. Rosseinsky, S. J. Blundell, P. D. Battle, M. Diaz, I. Uriarte, and T. Rojo, Phys. Rev. B **83**, 104404 (2011).
[12] J. Lago *et al*., (unpublished).
[13] T. Takeda, T. Watanabe, S. Komura, and S. Fujii, J. Phys. Soc. Jpn. **56**, 731 (1987).
[14] S. J. Blundell, Contemp. Phys. **40**, 175 (1999); P. Dalmas de Reotier and A. Yaouanc, J. Phys.: Condens. Matter **9**, 43 (1997); A. Yaouanc and P. Dalmas de Reotier, *Muon Spin Rotation, Relaxation, and Resonance: Applications to Condensed Matter* (Oxford University Press, Oxford, 2010).
[15] I. A. Campbell, A. Amato, F. N. Gygax, D. Herlach, A. Schenck, R. Cywinski, and S. H. Kilcoyne, Phys. Rev. Lett. **72**, 1291 (1994); A. T. Ogielski, Phys. Rev. B **32**, 7384 (1985).
[16] J. A. Mydosh, *Spin Glasses. An Experimental Introduction* (Taylor & Francis, London, 1993); K. Binder and A. Young, Rev. Mod. Phys. **58**, 801 (1986).
[17] L. Lundgren, P. Svedlindh, P. Nordblad, and O. Beckman, Phys. Rev. Lett. **51**, 911 (1983).
[18] E. Vincent, Lect. Notes Phys. **716**, 7 (2007).
[19] D. S. Fisher and D. A. Huse, Phys. Rev. Lett. **56**, 1601 (1986); Phys. Rev. B **38**, 386 (1988).
[20] F. Rivadulla, M. A. López-Quintela, and J. Rivas, Phys. Rev. Lett. **93**, 167206 (2004).
[21] S. Sahoo, O. Petracic, W. Kleemann, P. Nordblad, S. Cardoso, and P. P. Freitas, Phys. Rev. B **67**, 214422 (2003); D. Parker, V. Dupuis, F. Ladieu, J.-P. Bouchaud, E. Dubois, R. Perzynski, and E. Vincent *ibid*. **77**, 104428 (2008).
[22] J. L. Tholence, Physica B + C **126**, 157 (1984); T. Mori and H. Mamiya, Phys. Rev. B **68**, 214422 (2003); R. J. Tackett, J. G. Parsons, B. I. Machado, S. M. Gaytan, L. E. Murr, and C. E. Botez, Nanotechnology **21**, 365703 (2010).
[23] C. Tien, C. H. Feng, C. S. Wur, and J. J. Lu, Phys. Rev. B **61**, 12151 (2000); A. Malinowski, V. L. Bezusyy, R. Minikayev, P. Dziawa, Y. Syryanyy, and M. Sawicki, *ibid*. **84**, 024409 (2011).
[24] P. C. Hohenberg and B. I. Halperin, Rev. Mod. Phys. **49**, 435 (1977); R. Laiho, E. Lähderanta, J. Salminen, K. G. Lisunov, and V. S. Zakhvalinskii, Phys. Rev. B **63**, 094405 (2001).
[25] T. Klimczuk, H. W. Zandbergen, Q. Huang, T. M. McQueen, F. Ronning, B. Kusz, J. D. Thompson, and R. J. Cava, J. Phys.: Condens. Matter **21**, 105801 (2009); R. N. Bhowmik and R. Ranganathan, J. Magn. Magn. Mater. **248**, 101 (2002).
[26] J. L. Tholence, Solid State Commun. **35**, 113 (1980).
[27] J. Souletie and J. L. Tholence, Phys. Rev. B **32**, 516 (1985).
[28] Y. Yeshurun, J. L. Tholence, J. K. Kjems, and B. Wanklyn, J. Phys. C **18**, L483 (1985).
[29] D. Fiorani, J. L. Tholence, and J. L. Dormann, J. Phys. C **19**, 1945 (1986).
[30] K. H. Fisher and J. A. Hertz, *Spin Glasses* (Cambridge University Press, Cambridge, 1991).
[31] M. Suzuki, Prog. Theor. Phys. **58**, 1151 (1977).
[32] J. Chalupa, Solid State Commun. **22**, 315 (1977).
[33] A. Mauger, J. Ferré, and P. Beauvillain, Phys. Rev. B **40**, 862 (1989).
[34] L. P. Lévy and A. T. Ogielski, Phys. Rev. Lett. **57**, 3288 (1986); H. Bouchiat, J. Phys. (Paris) **47**, 71 (1986); N. de Courtenay, H. Bouchiat, H. Hurdequint, and A. Fert, *ibid*. **47**, 1507 (1986); T. Taniguchi and Y. Miyako, J. Phys. Soc. Jpn. **57**, 3520 (1988); T. Taniguchi, J. Phys.: Condens. Matter **19**, 145213 (2007); T. Taniguchi and K. Makisaka, J. Phys.: Conf. Ser. **320**, 012046 (2011).
[35] K. Hukushima and H. Kawamura, Phys. Rev. B **72**, 144416 (2005); D. X. Viet and H. Kawamura, *ibid*. **80**, 064418 (2009); I. A. Campbell and D. C. M. C. Petit, J. Phys. Soc. Jpn. **79**, 011006 (2010).
[36] J. de Almeida and D. J. Thouless, J. Phys. A **11**, 983 (1978).
[37] D. Sherrington and S. Kirkpatrick, Phys. Rev. Lett. **35**, 1792 (1975).
[38] S. F. Edwards and P. W. Anderson, J. Phys. F **5**, 965 (1975).
[39] M. Gabay and G. Toulouse, Phys. Rev. Lett. **47**, 201 (1981).
[40] G. Parisi, Phys. Rev. Lett. **43**, 1754 (1979); **50**, 1946 (1983).
[41] G. Kotliar and H. Sompolinsky, Phys. Rev. Lett. **53**, 1751 (1984); K. H. Fisher, Z. Phys. B **60**, 151 (1985).
[42] G. G. Kenning, D. Chu, and R. Orbach, Phys. Rev. Lett. **66**, 2923 (1991); F. Lefloch, J. Hammann, M. Ocio, and E. Vicent, Phys. B **203**, 63 (1994); F. Bernardot and C. Rigaux, Phys. Rev. B **56**, 2328 (1997); D. Petit, L. Fruchter, and I. A. Campbell, Phys. Rev. Lett. **88**, 207206 (2002).
[43] J. R. Banavar and M. Cieplak, Phys. Rev. Lett. **48**, 832 (1982); J. A. Olive, A. P. Young, and D. Sherrington, Phys. Rev. B **34**, 6341 (1986).
[44] H. Kawamura, Phys. Rev. Lett. **68**, 3785 (1992).
[45] H. Kawamura, J. Phys. Soc. Jpn. **79**, 011007 (2010).
[46] F. Matsubara, T. Shirakura, and S. Endoh, Phys. Rev. B **64**, 092412 (2001); T. Nakamura and S. Endoh, J. Phys. Soc. Jpn. **71**, 2113 (2002); I. Campos, M. Cotallo-Aban, V. Martin-Mayor, S. Perez-Gaviro, and A. Tarancon, Phys. Rev. Lett. **97**, 217204 (2006); A. P. Young, J. Phys.: Conf. Ser. **95**, 012003 (2008).
[47] D. Imagawa and H. Kawamura, J. Phys. Soc. Jpn. **71**, 127 (2002).
[48] I. Maksimov, F. J. Litterst, D. Menzel, J. Schoenes, A. A. Menovsky, J. Mydosh, and S. Süllow, Phys. B **312**, 289 (2002).
[49] E. Vincent and J. Hammann, J. Phys. C **20**, 2659 (1987).
[50] Note that although longitudinal magnetization measurements such as those presented in this work have been used in the past to determine the *H-T* phase diagram in spin glasses (see Ref. 42), the validity of this approach has been disputed by other authors[51] according to which it is only torque measurements—providing direct information about the transverse magnetization–that can reliably establish the position of the weak irreversibility (GT) line in the phase diagram. In that sense, torque measurements of the current system would provide a definitive confirmation of the reported in-field behavior.
[51] D. Petit, L. Fruchter, and I. A. Campbell, Phys. Rev. Lett. **83**, 5130 (1999).